HYDROLOGICAL PROCESSES
Hydrol. Process. **20**, 3555–3566 (2006)
Published online 24 April 2006 in Wiley InterScience (www.interscience.wiley.com). DOI: 10.1002/hyp.6145

Assessing the geochemical reactivity of inorganic phosphorus along estuaries by means of laboratory simulation experiments

Enrique García-Luque,* Jesús M. Forja Pajares and Abelardo Gómez-Parra
Departamento de Química Física, Facultad de Ciencias del Mar y Ambientales, Universidad de Cádiz, Campus Río San Pedro s/n 11510 Puerto Real, Cádiz, Spain

Abstract:

Phosphate behaviour in natural estuarine systems can be studied by performing field measurements and by undertaking laboratory simulation experiments. Thus, in this paper we describe the use of a dynamic automated estuarine simulator to characterize the geochemical reactivity of phosphate in varying salinity gradients in order to study possible mechanisms of phosphate removal from the dissolved phase (e.g. formation of some kind of apatite) and how changes in pH and salinity values influence this removal. Six laboratory assays, representing various salinity and pH gradients (average pH values between 7 and 8), were carried out. The geochemical equilibrium model MINTEQA2 was employed to characterize removal of phosphate. Among the minerals from which dissolved phosphate can originate, it seems that hydroxyapatite is by far the mineral that shows the greatest saturation indexes in the experiments. Thus, there is evidence that a type of calcium phosphate (hydroxyapatite) is involved in phosphate removal in the assays. Phosphate removal by Ca^{2+} occurs sharply at salinity values of 1–2, whereas by Fe^{3+} it is relatively gradual, at least until a salinity value of 7. Copyright © 2006 John Wiley & Sons, Ltd.

KEY WORDS phosphate; simulation; MINTEQ; estuaries

INTRODUCTION

Phosphate behaviour in natural estuarine systems can be studied by performing field measurements, and by undertaking laboratory simulations. While acknowledging the need to work on site for these types of study, simulations can significantly reduce the amount of field survey work to be carried out. Logically, results obtained by means of simulation need to be validated by comparison with field measurements.

In addition, laboratory simulation offers other advantages over fieldwork: by controlling in the laboratory the desired environmental conditions, it is possible to reproduce certain processes that occur only sporadically or unpredictably in the field.

The dynamic simulation of real estuaries was first carried out by Bale and Morris (1981) and applied to studies of phosphate and iron reactivity in the Tamar estuary. Doering *et al*. (1995) also used this technique to evaluate biological activity in estuarine systems. Nevertheless, the dimensions and the features offered by the simulator employed in this study are considerably greater. The principal improvement is the remote control of the equipment by means of a computer system. Simulation under static conditions has been used more frequently (Preston and Riley, 1982; Bilinski *et al*., 1991; Turner *et al*., 1993).

In relation to phosphorus geochemical reactivity in natural estuaries, Lebo (1991) reported on the phosphorus behaviour in Delaware estuary, which is typical of many estuaries (e.g. Shengquan, 1993; Bay of Hangzhou). The highest phosphorus concentration appears in the fluvial area of the estuary, the nearest zone to

* Correspondence to: Enrique García-Luque, Dpto. de Química Física, Facultad de Ciencias del Mar y Ambientales, Universidad de Cádiz, Campus Río San Pedro s/n, 11510 Puerta Real, Cádiz, Spain. E-mail: enrique.luque@uca.es

Received 16 November 2004
Accepted 12 August 2005

anthropogenic discharges, with lower values appearing in the mixed zone. Analysis revealed that particulate phosphorus was associated with the particulate organic matter, oxides of aluminium and iron and apatite during its formation. Near the marine limit of the estuary, the fraction of phosphorus associated with metallic oxides decreased with the increase in salinity, whereas changes in the fraction of apatitic phosphorus were not found (Tanaka, 1995). In fact, there are results that suggest that formation and retention of authigenic apatite is the predominant process for phosphorus removal from the coastal biogeochemical cycle (Van Beusekom and De Jonge, 1997).

Many studies show that the interaction between inorganic phosphorus and particulate matter represents one of the most important mechanisms affecting the geochemical phosphorus levels in estuarine systems (Froelich, 1988; Balls, 1994; Conley *et al*., 1995). The kinetics of phosphate removal by minerals, under conditions of low salinity, suggest that adsorption is the principal process of phosphate removal. Others (Carritt and Goodgal, 1954; Burns and Salomons, 1969) have determined the optimum pH for phosphate adsorption, showing an extensive interval spanning values between pH 3 and 7. Within this interval, the main dissolved phosphorus species present is $H_2PO_4^-$ according to dissociation curves of phosphoric acid proposed by Kester and Pytkowicz (1967). In seawater, with pH values around 8, only 1% of dissolved phosphorus exists as $H_2PO_4^-$, with the predominant species being $H_2PO_4^{2-}$ (87%). These experimental results imply that in an estuary, in which fresh water (with lower pH values) mixes with seawater (with pH $\sim$ 8), the efficiency of phosphorus removal from the dissolved phase is higher in the 'fluvial area' of the estuary. Carritt and Goodgal (1954) and Burns and Salomons (1969) showed that, for a fixed value of pH, a salinity increment along a gradient involves a decrease of phosphate removal from the dissolved phase. This may be due to the blocking of the preferential adsorption centres by ions like Cl^- and SO_4^{2-}.

Thus, in this paper we describe the use of a dynamic automated estuarine simulator to characterize the geochemical reactivity of phosphate along different salinity gradients in order to study possible mechanisms of phosphate removal from the dissolved phase (e.g. formation of some kind of apatite) and how changes in pH and salinity influence this removal.

MATERIAL AND METHODS

Simulator description

Basically, the simulation of estuarine mixing is achieved by the cross-current mixing of seawater with river water (Figure 1). The mixture is performed in a series of eight tanks (Plexiglass, cylindrical, and of about 12 l capacity) interconnected under a hydrodynamic regime and situated at ascending levels. The lowest tank is supplied with seawater and the highest tank is supplied with freshwater. From the lower to the upper tanks, there is a forced flow of water controlled by peristaltic pumps. In the inverse direction, filling the containers in series with freshwater generates a downward flow. This permits a constant volume of 10 l to be maintained in each tank.

The temperature in each tank is controlled by means of coated dip heaters. The flow and temperature control is carried out by a personal computer using an AID 21-bit translation card. The regulation of flow involves setting up the peristaltic pumps (Masterflex, 7521-55) in phase with the flow meters (McMillan Company, 111). To ensure a homogeneous mixture of both types of water, variable-velocity mechanical stirrers are used. The tanks are aerated by means of a blower system, with submerged diffusers, to ensure the correct oxygenation of the water in all the simulations performed. A more detailed description of this system can be found in García-Luque *et al*. (2003).

Experiments are conducted over an 8-day period, so as to ensure that the adsorption onto tank walls is produced in the first hours and its influence on the phosphate concentration at the end of the experiment is negligible.

By choosing appropriate relationships between the flows, it is possible to generate a large number of longitudinal salinity gradients similar to those in real estuaries. Conceptually, the simulation of the process

of mixing in the estuary consists of substituting the continuous variation in salinity that is produced in a real estuary by a series of stages in each of which the salinity is constant, and between which there exists a sharp variation in the salinity.

Description of the experiments

To assess phosphate geochemical reactivity in estuarine sediments, two sets of experiments were carried out: experiments 1, 2 and 3 simulate complete salinity gradients and experiments 4, 5 and 6 simulate the zone of low salinity values (enlargement of the fluvial area of the estuary).

Seawater was collected in a clean coastal area of the Bay of Cádiz and filtered to 1 μM. Table I shows the chemical composition of this water. Conversely, freshwater was synthetically prepared following the protocol described by Millero and Sohn (1992) to obtain a river water of standard composition ($NaHCO_3$ (0·95 mM), $MgCl_2{\cdot}6H_2O$ (0·15 mM), K_2SO_4 (0·10 mM), $CaCl_2{\cdot}2H_2O$ (0·40 mM), Na_2HPO_4 (50 μ M/10 μ M)).

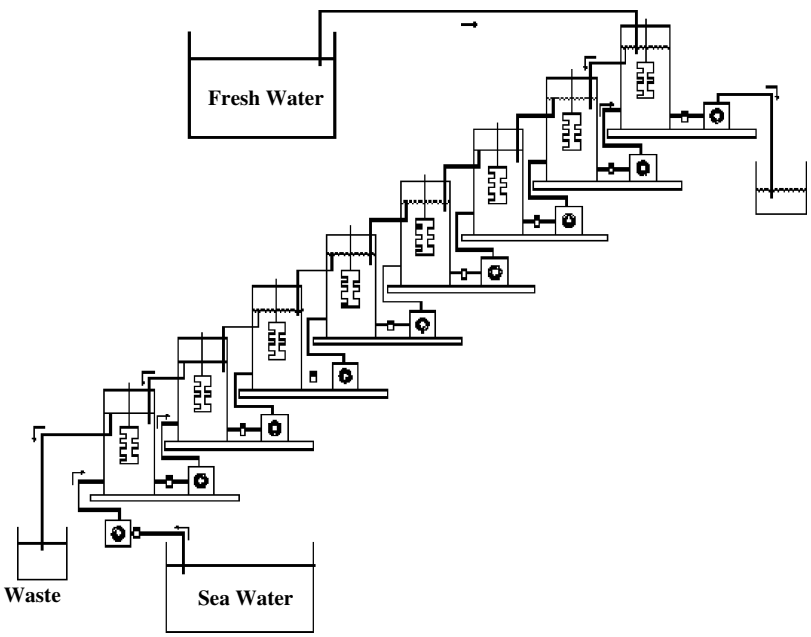

Figure 1. Schematic representation of the estuarine hydrodynamic simulation system (adapted from García-Luque *et al*. (2003))

Table I. Chemical composition of the seawater employed in the simulations experiments

Salinity	37·098
pH	8·124
Inorganic carbon (mM)	2·271
Dissolved oxygen (mg L^{-1})	5·66
Chloride (mM)	598·91
Sulfate (mM)	31·36
Calcium (mM)	9·70
Ammonium (μM)	3·3
Nitrite (μM)	0·8
Nitrate (μM)	2·0
Phosphate (μM)	2·5
Silicate (μM)	6·6

A phosphate concentration of 50 μM in the freshwater was employed for experiments 1, 2 and 3. In addition, for experiments 2 and 3, freshwater was acidified (by addition of HCl) to establish different pH gradients. The average pH for experiments 1 and 2 was around 8, whereas in experiment 3 the pH was close to 7.

For experiments 4, 5 and 6, a phosphate concentration of 10 μM in the freshwater was employed. This value is similar to those found in natural systems. Salinity gradient in experiment 4 ranged from 0 to 10. In experiment 5 the salinity ranged from 0 to 5, whereas in experiment 6, the range was from 0 to 10 once again. However, in this experiment (6) an iron concentration of 5 μM was added to the freshwater to assess the effect of the presence of iron on apatite formation, since iron competes with calcium in the processes of phosphate adsorption. The average pH values for experiments 4 and 5 were 7·9 and 7·4 respectively, whereas for experiment 6 the pH was 7·0. The average duration for these experiments was 8·5 days.

Analytical techniques

Three phosphate fractions were quantified experimentally by means of spectrophotometric techniques: total, dissolved and particulate phosphate. Total phosphate was measured in unfiltered samples from each tank. Dissolved phosphate was measured in filtered samples using a 0·22 μM filter (GSWPO-2500, Millipore). The particulate phosphate accumulated was quantified for the filters employed in each tank. In all cases, the methodology employed for phosphate determination was that described by Grasshoff *et al*. (1983).

All samples were stored in the dark at 4 °C until their analysis. In all cases, the sample analysis began within 3 days following their collection. Three replicates of each sample were made.

The salinity of the samples was determined by means of an induction salinometer (Beckman, RS-10). The initial pH (NBS) and the inorganic carbon content were measured by potentiometric titration (Metrohm, 670). The sulphate concentration was determined by gravimetry (Grasshoff *et al*., 1983). Chlorinity was determined by silver potentiometric titration. The concentration of calcium in the containers was analysed by flame atomic absorption spectrophotometry using matrix correctors.

RESULTS AND DISCUSSION

Figure 2 shows the variation of dissolved phosphate concentration along salinity gradients simulated in experiments 1, 2 and 3. As expected, phosphate behaved in a non-conservative manner, along the same lines as results obtained in a number of publications related to phosphate behaviour (e.g. Bale and Morris, 1981; Lebo, 1991; Prastka *et al*., 1998; Fang, 2000).

The zone of highest reactivity was found at low salinity values, in the 'fluvial' area of the simulated estuaries, where the most pronounced deviations from the theoretical dilution line (the line that joins the points of the concentrations of phosphate in the sea and in the river) were obtained. These experiments revealed the need to focus on the lower salinity values in the subsequent simulations (experiments 4, 5 and 6) in order to characterize phosphate geochemical reactivity best.

Losses of phosphate from the dissolved phase were quantified for the six experiments, following the procedure described by Ortega *et al*. (2001). For this, it is only necessary to obtain the difference between the flow of phosphate across the two sections delimiting the estuary employing the expression $L(\mathrm{P}) = (100/C_0)[C - S(\mathrm{d}C/\mathrm{d}S)]$. C_0 is the total quantity of phosphate supplied by the river and it is only necessary to know the concentration of phosphate and the salinity at the extremes of the stretch and the values of the derivate $C = f(S)$ at these salinity points. In all cases, the highest losses appeared in the area of low salinity values (below a salinity value of 3; from this value, losses decreased gradually as the salinity increased). The average value of phosphate losses at salinities below 3 (for all experiments) was 60·5% in relation to total losses. Müller-Karulis (1999) found that phosphate removal at low salinity values reaches up to 70% of total phosphate supplied by the river.

Although loss quantification supplies information about phosphate total reactivity under experimental conditions, it does not permit us to establish the most probable mechanisms of phosphate removal. Thus,

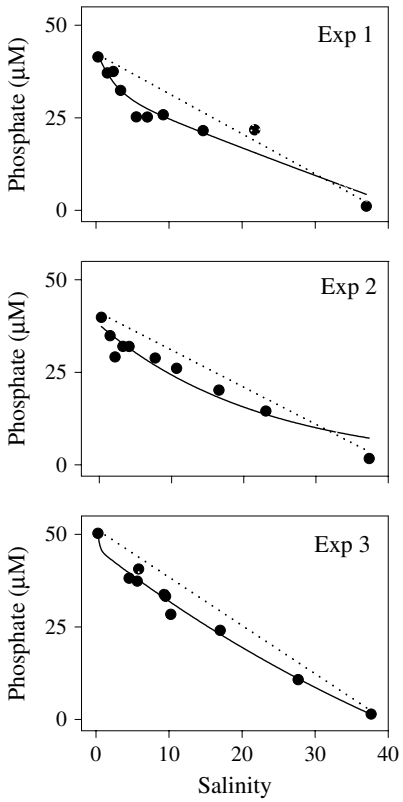

Figure 2. Variation of the phosphate concentrations along the salinity gradients simulated in experiments 1, 2 and 3. Solid curved lines represent the predicted values by the exponential decay approach; dashed line represents the theoretical dilution line in each experiment

a geochemical equilibrium model was employed to find, in a theoretical way, the feasible reactions that a chemical species may be involved in (knowing the composition of the solution). Results from this program may be useful for the interpretation of phosphate geochemical reactivity, at least from a comparative viewpoint amongst the experiments carried out. We used the geochemical equilibrium model MINTEQA2 (Allison *et al*., 1991), frequently employed to assess chemical speciation and solubility equilibrium in aqueous solutions. In fact, some workers (e.g. Lee *et al*., 2003) have employed this program to characterize removal of nitrogen and phosphate, specifically, from wastewater. This program uses an extensive database of thermodynamic constants (and different approximations to assess the influence of temperature and ionic strength on these constants). Several workers use this kind of thermodynamic geochemical model to simulate trace element behaviour in natural waters, comparing the results obtained with field measurements (e.g. Bruno *et al*., 2002). Thus, it is possible to calculate the supersaturation of the minerals in the water, assessing their trend to precipitate by means of saturation indexes.

Saturation index Ω is the logarithmic relation between ionic activity product (IAP) and the solid formation constant K:

$$\Omega = \log \frac{\mathrm{IAP}}{K}$$

Thus, if $\Omega > 0$, then the thermodynamic trend is toward compound precipitation.

We used experimental values of pH, temperature, ionic strength, inorganic carbon, sulphate, chloride, calcium and phosphate of samples from each tank of the simulator. Since relations between the majority of

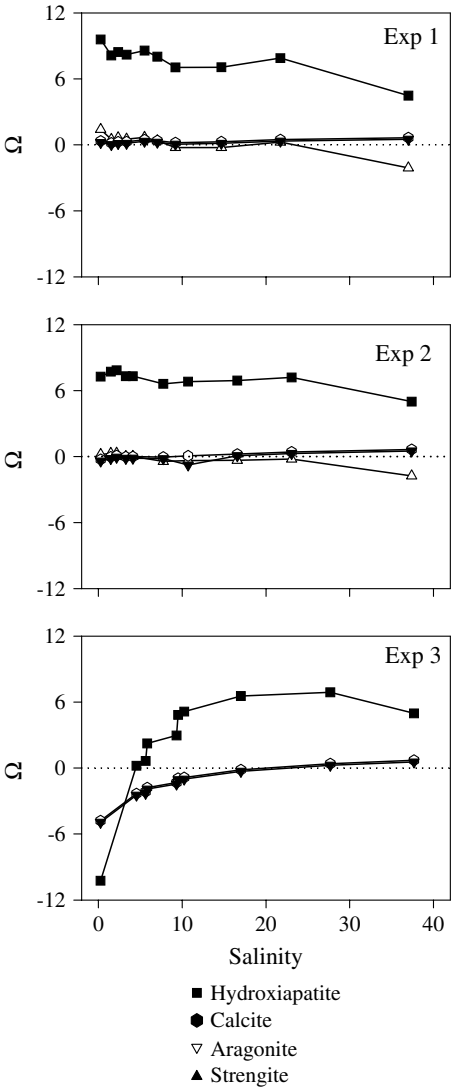

Figure 3. Variations of the saturation indexes versus salinity values for all mineral phases apparently involved in the phosphate geochemical reactivity for experiments 1, 2 and 3

elements remain constant in seawater (Millero and Sohn, 1992), total concentrations of potassium, sodium and magnesium were estimated for all samples analysed.

Figure 3 shows variations in saturation indexes with salinity for all mineral phases involved in the geochemical reactivity of phosphate for experiments 1, 2 and 3. The three experiments show supersaturation in relation to the hydroxyapatite formation ($Ca_5(PO_4)_3(OH)$).

The saturation index for hydroxyapatite tended to decrease as salinity increased, being elevated in all cases (between 4 and 8) with the exception of experiment 3, in which the saturation index was negative at the fluvial zone of the estuary, tending to rise as salinity increased (probably due to the lower pH gradient imposed in this experiment).

Experiments 1 and 2 also displayed supersaturation in relation to whitlockite (β-$Ca_3(PO_4)_2$) for salinities of up to 5. Saturation index values were lower than for those of hydroxyapatite.

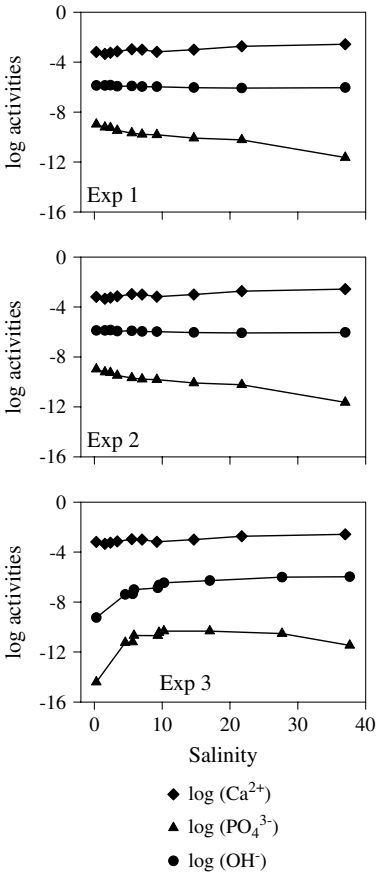

Figure 4. Logarithm of activities of Ca^{2+}, PO_4^{3-} and OH^- versus salinity gradient for experiments 1, 2 and 3

In addition, it was found that saturation indexes were slightly positive for other insoluble compounds (aragonite and calcite). This is in agreement with Ortega (2001, personal communication), who calculated the saturation of these minerals from empirical relations of solubility in relation to salinity and temperature, as well as with other authors' results for coastal systems (Giordani and Hammond, 1985; Barbanti *et al*., 1995).

Among the minerals from which dissolved phosphate originates, hydroxyapatite showed by far the greatest saturation indexes of the three experiments.

Hydroxyapatite is composed of Ca^{2+}, PO_4^{3-} and OH^- ions. Figure 4 shows the logarithm of the activities of these species versus salinity for the three experiments. Activity of Ca^{2+} increases with salinity in all cases, showing a trend opposite to that of the saturation index (Figure 3). Conversely, the variations in the activities of PO_4^{3-} and OH^- are similar to those of the saturation indexes. Thus, the tendency to form hydroxyapatite seems related to the variation in the concentration of these two species. Lower saturation index values in experiment 3 than those in experiments 1 and 2 look to be related to the pH gradient in this experiment. Saturation index varied with salinity values in a distinct way in experiment 3 when compared with experiments 1 and 2. The average pH for experiments 1 and 2 was around 8, whereas in experiment 3 the pH was close to 7. This diminution in pH affects the availability of OH^- ions and influences the percentage of phosphate available as PO_4^{3-}. Thus, pH is responsible for the saturation index variations found for experiment 3.

Phosphate was more reactive at low salinity. For this reason, three new experiments (4, 5 and 6) were carried out. The aim of these experiments was to focus on the zone of low salinity values.

Figure 5 depicts the variations in the concentrations of dissolved and particulate phosphate along the salinity gradient in experiments 4, 5 and 6. Again, concentration of dissolved phosphate does not show a linear variation with salinity values, due to geochemical reactivity. Therefore, phosphate displayed the same non-conservative behaviour as that extensively described by others (e.g. Rendell *et al.*, 1997; Fang, 2000).

In experiments 4, 5 and 6, variations in the concentration of dissolved phosphate with salinity are described by the following quadratic equation:

$$C = a + bS + cS^2$$

where C is the concentration of dissolved inorganic phosphate, S is the salinity, and a, b, and c are the fitted parameters for each experiment. Table II shows the values for the fitted parameters,

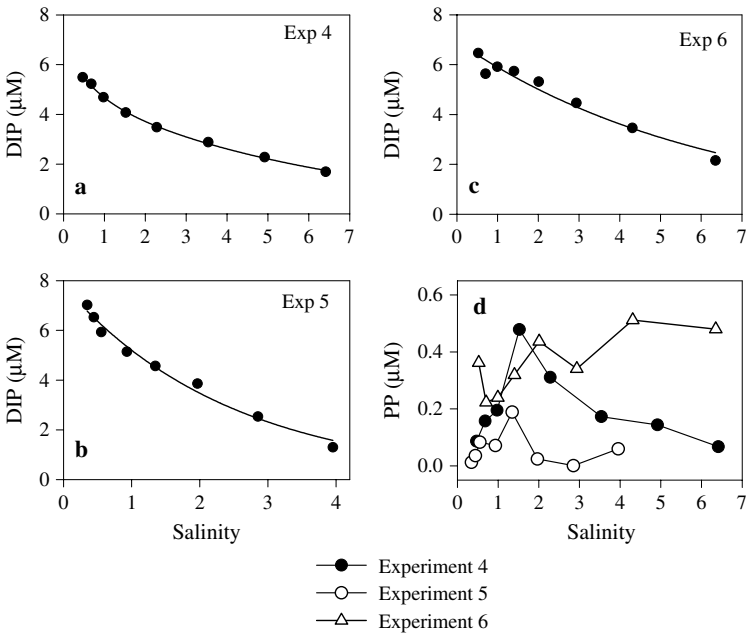

Figure 5. Variation of the dissolved inorganic phosphate (DIP) concentrations along the salinity gradients simulated in (a) experiment 4, (b) experiment 5, and (c) experiment 6. Solid curved lines represent the predicted values for DIP by the exponential decay approach. (d) Variation of the particulate phosphorus (PP) concentrations along the salinity gradients simulated in experiments 4, 5 and 6

Table II. Fitted parameters (a, b, and c), standard errors, significance levels P and coefficients of correlation r^2 for variation of the concentration of dissolved phosphate with salinity for experiment 4, 5 and 6

Experiment no.	Parameter		Standard error	P	r^2
4	a	5·8834	0·1626	<0·0001	
	b	−1·1902	0·1349	0·0003	0·989
	c	0·0862	0·0198	0·0074	
5	a	7·4399	0·2570	<0·0001	
	b	−2·3246	0·3413	0·0010	0·986
	c	0·1999	0·0807	0·0560	
6	a	6·5895	0·2369	<0·0001	
	b	−7·7099	0·1958	0·0151	0·978
	c	0·0009	0·0286	0·9763	

as well as the coefficient of correlation, the standard error and the significance level for the three assays.

In relation to the variation in particulate phosphate along the salinity gradient for experiments 4, 5 and 6, Figure 5 shows that experiment 6 displayed the highest concentrations. This is reasonable, since phosphate removal from the dissolved phase in this assay may have been due to its reaction with Ca^{2+} and Fe^{3+}, whereas in experiments 4 and 5 the phosphate was only able to react with Ca^{2+}. Phosphate removal by Ca^{2+} occurs sharply at salinity values of 1–2, whereas it is relatively gradual by Fe^{3+}, at least until a salinity value of 7.

Figure 6 shows the variation of the saturation index with salinity (calculated by means of MINTEQA2) for mineral phases involved in experiments 4, 5 and 6. Supersaturation of hydroxyapatite was found in all experiments, whereas strengite was found only in experiment 6 (owing to the presence of iron). Forms of calcium carbonate were present in experiments 4 and 6. In these three cases, the saturation index of

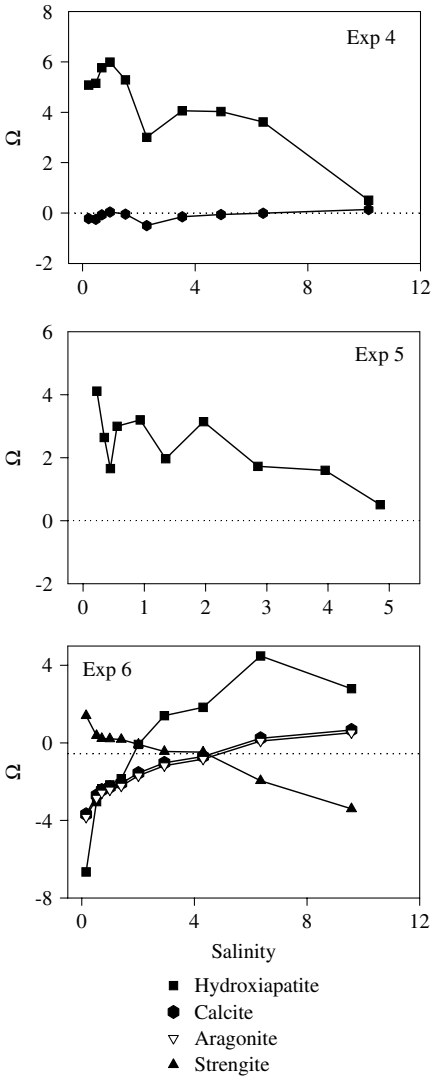

Figure 6. Variations of the saturation indexes versus salinity values for all mineral phases apparently involved in the phosphate geochemical reactivity for experiments 4, 5 and 6

hydroxyapatite was lower than that found in experiments 1, 2 and 3. This was due to the concentration of phosphate employed in assays 1, 2 and 3 being five times that employed in experiments 4, 5 and 6.

The behaviour of hydroxyapatite saturation index in experiments 4 and 5 was similar (taking into account the fact that the salinity range in experiment 4 was broader than that used in experiment 5). Saturation index values in experiment 5 were lower than for experiment 4 due to the varying pH gradient simulated in each assay. Nevertheless, the saturation index values were positive at all salinities in both experiments. The average pH values for experiments 4 and 5 were 7·9 and 7·4 respectively, whereas for experiment 6 the pH was 7·0.

Saturation index values of hydroxyapatite in experiment 6 were negative up to a salinity of close to 2; thereafter, they increased until reaching a saturation index of around 3·5. In this case, dissolved phosphate, in addition to taking part in the hydroxyapatite formation, may participate in strengite formation (owing to the Fe^{3+} presence in this assay). In fact, the behaviour of the strengite saturation index is opposite to that of hydroxyapatite. The low saturation indexes in experiment 6 are related to the gradient of pH simulated in this assay.

In experiments 4, 5 and 6, supersaturation of some calcium minerals (such as aragonite and calcite) was found. In experiment 6, ferric minerals (such as goethite and haematite) common in real estuaries were also found. Despite this, in all cases, these minerals showed supersaturated values, near equilibrium, along all salinity gradients.

Figure 7 shows the logarithm of the activities of the ions involved in hydroxyapatite formation and the logarithm of the IAP of the hydroxyapatite versus salinity for experiments 4, 5 and 6 (for experiment 6, the same variations related to strengite formation are included). In the three cases, Ca^{2+} behaved in a similar way, with its activity values oscillating around the same values. Therefore, it is not the species that influences the varying hydroxyapatite in the three experiments. Activities of PO_4^{3-} and OH^- behaved similarly in experiments 4 and 5. Hydroxyapatite evolution was analogous in both experiments, but distinct to that seen

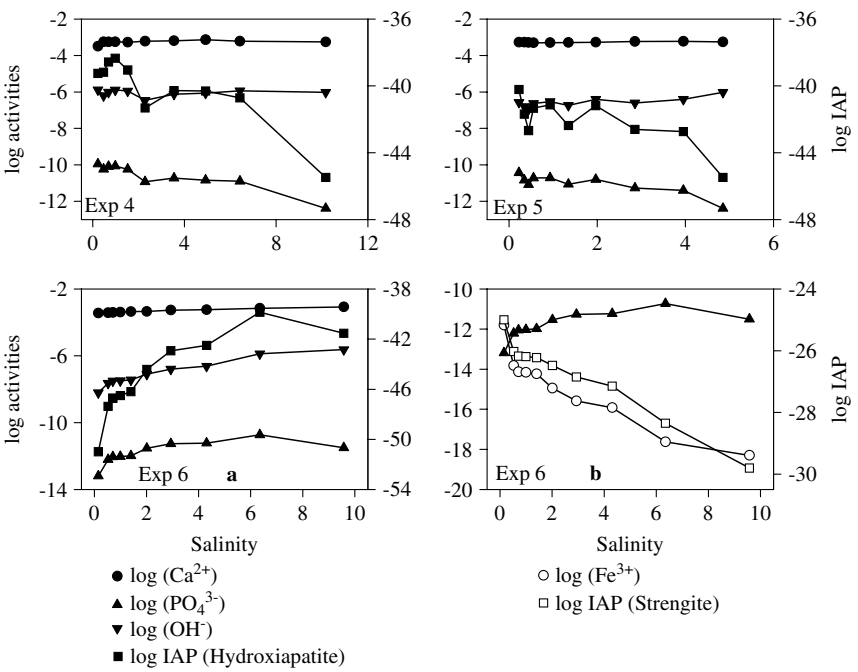

Figure 7. (a) Logarithm of activities of Ca^{2+}, PO_4^{3-} and OH^- and logarithm of the ionic activity product (IAP) of hydroxyapatite versus salinity gradient for experiments 4, 5 and 6. (b) Logarithms of activities PO_4^{3-} and Fe^{3+} and logarithm of the ionic activity product (IAP) of strengite in experiment 6

in experiment 6. Therefore, both chemical species are responsible (although not exclusively) for the distinct hydroxyapatite behaviour in the final experiment. In experiment 6, phosphate is divided between potential formation of hydroxyapatite and strengite, mainly at low salinities, where Fe^{3+} activity was seen to surpass that of PO_4^{3-}.

CONCLUSIONS

The device employed allows the simulation in a realistic manner of the chemical reactivity of substances (like phosphorus) passing through an estuary, constituting a useful tool that avoids many of the logistical problems involved with *in situ* surveys. Logically, results obtained by means of simulation need to be validated by comparison with field measurements. Aside from this, the simulator is also useful for carrying out *a priori* environmental risk assessments, introducing the desired pollutants to the river water or to whichever of the tanks that represent the specific zone of the estuary involved.

With regard to the experiments described in this work, it seems that within the group of minerals that dissolved phosphate can originate, hydroxyapatite is the mineral that shows by far the greatest saturation indexes in the experiments. Thus, there is evidence that a type of calcium phosphate (hydroxyapatite) may be involved in the phosphate removal in the laboratory assays undertaken. In the presence of iron, strengite may also contribute to the removal process. Nevertheless, further studies are required to establish the most probable mechanisms of phosphate removal.

REFERENCES

Allison JD, Brown DS, Novo-Gradac KJ. 1991. *MINTEQA2/PRODEFA2: a geochemical assessment model for environmental systems: version 3·0 user's manual*. US EPA, Environmental Research Laboratory. EPA/600/3-91/021.

Bale AJ, Morris AW. 1981. Laboratory simulation of chemical processes induced by estuarine mixing: the behaviour of iron and phosphate in estuaries. *Estuarine, Coastal and Shelf Science* **13**: 1–10.

Balls PW. 1994. Nutrient inputs to estuaries from nine Scottish east coast rivers: influence of estuarine processes on inputs to the North Sea. *Estuarine, Coastal and Shelf Science* **39**: 329–352.

Barbanti A, Bergamini MC, Frascari F, Miserocchi S, Ratta M, Rosso G. 1995. Diagenetic processes and nutrient fluxes at the sediment–water interface, northern Adriatic Sea, Italy. *Marine and Freshwater Research* **46**: 55–67.

Bilinski H, Kozar S, Plavsic M, Kwokal Z, Branica M. 1991. Trace metal adsorption on inorganic solid phases under estuarine conditions. *Marine Chemistry* **32**: 225–233.

Bruno J, Duro L, Grivé M. 2002. The applicability and limitations of thermodynamic geochemical models to simulate trace element behaviour in natural waters. Lessons learned from natural analogue studies. *Chemical Geology* **190**: 371–393.

Burns PA, Salomon M. 1969. Phosphate adsorption by kaolin in saline environments. *Proceedings of the National Shellfisheries Association* **59**: 121–125.

Carrit DE, Goodgal S. 1954. Sorption reactions and some ecological implications. *Deep-Sea Research* **1**: 224–243.

Conley DJ, Smith PL, Cornwell EA, Fisher AL. 1995. Transformation on particle-bound phosphorus at the land–sea interface. *Estuarine, Coastal and Shelf Science* **40**: 161–176.

Doering PH, Oviatt CA, Nowicki BL, Klos EG, Reed LW. 1995. Phosphorus and nitrogen limitation of primary production and a simulated estuarine gradient. *Marine Ecology Progress Series* **124**: 271–287.

Fang TH. 2000. Partitioning and behaviour of different forms of phosphorus in the Tanshui estuary and one of its tributaries, north Taiwan. *Estuarine, Coastal and Shelf Science* **50**: 689–701.

Froelich PN. 1988. Kinetic control of dissolved phosphate in natural rivers and estuaries: a primer on the phosphate buffer mechanism. *Limnology and Oceanography* **33**: 649–688.

García-Luque E, Forja JM, DelValls TA, Gómez-Parra A. 2003. The behaviour of heavy metals from the Guadalquivir estuary after the Aznalcollar mining spill: field and laboratory surveys. *Environmental Monitoring and Assessment* **83**: 71–88.

Giordani P, Hammond DE. 1985. Techniques for measuring benthic fluxes of ^{222}Rn and nutrients in coastal waters. *Consiglio Nazionale delle Ricerche, Istituto per la Geologia Marina. Bologna, Rapporto Tecnico* **20**: 1–33.

Grasshoff K, Ehrhardt M, Kremling K. 1983. *Methods of Seawater Analysis*. Verlag Chemie: Weinheim.

Kester DR, Pytkowicz RM. 1967. Determination of the apparent dissociation constants of phosphoric acid in sea water. *Limnology and Oceanography* **12**: 243–252.

Lebo ME. 1991. Particle-bound phosphorus along an urbanized coastal plain estuary. *Marine Chemistry* **34**: 225–246.

Lee SI, Weon SY, Lee CW, Koopman B. 2003. Removal of nitrogen and phosphate from wastewater by addition of bittern. *Chemosphere* **51**: 265–271.

Millero FJ, Sohn ML. 1992. *Chemical Oceanography*. CRC Press: Boca Raton.

Müller-Karulis B. 1999. Transformations of riverine nutrients in the Daubava river plume (Gulf of Riga). *ICES Journal of Marine Science* **56**: 180–186.

Ortega T, Forja JM, Gómez-Parra A. 2001. Teaching estuarine chemical processes by laboratory simulation. *Journal of Chemical Education* **78**: 771–774.

Prastka K, Sanders R, Jickells J. 1998. Has the role of estuaries as sources or sinks of dissolved inorganic phosphorus changed over time? Results of a K_D study. *Marine Pollution Bulletin* **36**: 718–728.

Preston MR, Riley JP. 1982. The interactions of humic compounds with electrolytes and three clay minerals under simulated estuarine conditions. *Estuarine, Coastal and Shelf Science* **14**: 567–576.

Rendell AR, Horrobin TM, Jickells TD, Edmuns HM, Brown J, Malcom SJ. 1997. Nutrient cycling in the Great Ouse estuary and its impact on nutrient fluxes to the Wash, England. *Estuarine, Coastal and Shelf Science* **45**: 653–668.

Shengquan G, Guohui H, Yuhen W. 1993. Distributional features and fluxes of dissolved nitrogen, phosphorus and silicon in the Hangzhou Bay. *Marine Chemistry* **43**: 65–82.

Tanaka K. 1995. Runoff loadings and chemical forms of soil phosphorus from rivers in Japan during the high flow stages. *Japan Agricultural Research Quarterly* **29**: 223–229.

Turner A, Millward GE, Bale AJ, Morris AW. 1993. Application of the K_D concept to the study of trace metal removal and desorption during estuarine mixing. *Estuarine, Coastal and Shelf Science* **36**: 1–13.

Van Beusekom JEE, De Jonge VN. 1997. Transformation of phosphorus in the Wadden Sea: apatite formation. *German Journal of Hydrography* **49**: 297–305.

